AUTOMATIC DISPERSION EXTRACTION USING CONTINUOUS WAVELET TRANSFORM

Shuchin Aeron

Department of ECE, Boston University

Sandip Bose , Henri-Pierre Valero

Schlumberger-Doll Research, Cambridge MA

ABSTRACT

In this paper we present a novel framework for automatic extraction of dispersion characteristics from acoustic array data. Traditionally high resolution narrow-band array processing techniques such as Prony's polynomial method and forward backward matrix pencil method have been applied to this problem. Fundamentally these techniques extract the dispersion components frequency by frequency in the wavenumber-frequency transform domain of the array data. The dispersion curves are subsequently extracted by a supervised post processing and labelling of the extracted wavenumber estimates, making such an approach unsuitable for automated processing. Moreover, this frequency domain processing fails to exploit useful time information. In this paper we present a method that addresses both these issues. It consists in taking the continuous wavelet transform (CWT) of the array data and then applying a wide-band array processing technique based on a modified Radon transform on the resulting coefficients to extract the dispersion curve(s). The time information retained in the CWT domain is useful not only for separating the components present but also for extracting group slowness estimates. The latter help in the automated extraction of smooth dispersion curves. In this paper we will introduce this new method referred to as the Exponential Projected Radon Transform (EPRT) in the CWT domain and limit ourselves to the analysis for the case of one dispersive mode. We will apply the method to synthetic and real data sets and compare the performance with existing methods.

***Index Terms*—** Array Signal Processing, Signal Analysis, Parameter Estimation, Wavelet Transforms, Acoustic Applications

I. INTRODUCTION

Acoustic investigations around the borehole in oilfield applications require the extraction of dispersion information from the data that is generated by firing an acoustic source in the borehole and collecting waveform traces at an array of receivers on borehole sonic logging tools, [1]. Dispersion refers to the characteristic variation of the slowness (reciprocal of velocity) as well as attenuation of propagating waves as a function of the frequency and carries useful information about the rock formations around the borehole. Consequently the study of dispersion and its extraction has been a subject of intensive research posing theoretical as well as computational challenges in the geophysics community. Initial papers in this direction dealt with narrowband processing techniques that required significant post-processing efforts, see [2], [3] and references therein.

Recently there has been interest in the application of time frequency methods to this problem, see [4] and references therein. The approach presented here is also based on time-frequency representations but differs from the approach in [4] as discussed later. First we begin by outlining the problem set-up in the next section.

II. PROBLEM SET-UP

The waves that are generated in the borehole are recorded at a linear array of sonic receivers. The relation between the received waveforms and the frequency-wavenumber (ω-k) response of the borehole to the source excitation is captured via the following equation,

$$s(l,t) = \int_0^\infty \int_0^\infty X(f)Q(k,f)e^{i2\pi ft}e^{-ikz_l}\,df\,dk \qquad (1)$$

for $l = 1,2,...,L$ and where $s(l,t)$ denotes the pressure at time t at the l-th receiver located at a distance z_l from the source; $X(f)$ is the source spectrum and $Q(k,f)$ is the wavenumber-frequency response of the borehole. It has been shown that the complex integral in the wavenumber (k) domain can be approximated by the contribution due to the residues of the poles of the system response, [2]. Specifically,

$$\int_0^\infty Q(k,f)e^{-ikz_l}dk \sim \sum_{n=1}^{N(f)} a_n(f)e^{-(i2\pi k_n(f)+A_n(f))z_l} \qquad (2)$$

where $k_n(f)$ and $A_n(f)$ are the wavenumber and the attenuation as functions of frequency for the nth pole contribution (mode), $a_n(f)$ is the corresponding pole residue or amplitude factor and $N(f)$ is the number of significant modes. Then we have,

$$s(l,t) = \int_0^\infty \sum_{n=1}^{N(f)} X_n(f)e^{-(i2\pi k_n(f)+A_n(f))z_l}e^{i2\pi ft}df \qquad (3)$$

where $X_n(f) = X(f)a_n(f)$. Given the array data, the problem then is to estimate $k_n(f)$ and $A_n(f)$. We note that the slowness dispersion parameters, namely the phase slowness, s_ϕ, and group slowness, s_g, are functions of the wavenumber: $s_\phi = \frac{k(f)}{f}$, $s_g = \frac{\partial k(f)}{\partial f}$.

Typically in acoustic logging applications the number of receivers, L, is small, e.g. 10 receivers. Thus a simple 2-dimensional Fourier transform of the data does not result in a high resolution extraction of the dispersion parameters since the spatial sampling is very low leading to severe aliasing. In this paper we present high resolution methods for dispersion extraction for such scenarios.

For the sake of exposition, in this paper, we will focus on extraction of $k_n(f)$ and $A_n(f)$ when there is only one significant mode present. However, the method and the analysis shown here can be easily extended to multiple modes when they do not overlap in the time frequency plane. The main focus is to offer a method in continuous wavelet transform (CWT) domain for automated dispersion extraction of the phase and group slowness and the attenuation. We next outline this approach by establishing the formulation in the CWT domain.

III. DISPERSION EXTRACTION IN THE CWT DOMAIN

We begin with a brief review of the CWT; the reader is referred to [5] for more details. The CWT $S(a,b)$ of a function $s(t)$ is the scalar product of this signal by the dilated and translated wavelets from a family, given by $T^bD^a[g(t)] = \sqrt{a}g(\frac{t-b}{a})$, where $g(t)$ is the analyzing (mother) wavelet that is chosen to satisfy some admissibility condition [5]. The CWT at scale a and time shift b is given by

$$S(a,b) = \frac{1}{\sqrt{a}}\int s(t)g^*(\frac{t-b}{a})dt \qquad (4)$$

$$= \int_{-\infty}^{\infty} G^*(af)e^{i2\pi bf}S(f)df \qquad (5)$$

where $G(f)$ and $S(f)$ are the Fourier transforms of $g(t)$ and $s(t)$, the signal being analyzed, respectively.

Under the approximate model of equation (3) and restricting ourselves to the single mode case, the CWT at scale a and time shift b of the received waveforms is given by,

$$S_l(a,b) = \int_{-\infty}^{\infty} G^*(af)X(f)e^{i2\pi[bf-z_lk(f)]}e^{-z_lA(f)}df \qquad (6)$$

where we drop the indexing on n. In terms of inter-sensor spacing $\delta_{lj} = z_l - z_j$ between receiver l and j we can write,

$$S_l(a,b) = \int_{-\infty}^{\infty} G^*(af) S_j(f) e^{i2\pi[b-\delta_{lj}k(f)]} e^{-\delta_{lj}A(f)} df \quad (7)$$

where $S_j(f)$ is the Fourier transform of the waveform at receiver j. To begin with we write the local linear Taylor series expansion of $k(f)$ and $A(f)$ as

$$k(f) \approx k(f_a) + (f - f_a)k'(f_a) \quad (8)$$
$$A(f) = A(f_a) + o(|f - f_a|) \approx A(f_a) \quad (9)$$

where $f_a = \frac{\omega_0}{2\pi a}$ is the frequency corresponding to the scale a and related by the latter to the central frequency ω_0 of the mother wavelet. Under the above Taylor approximation we have,

$$\begin{aligned} S_l(a,b) &= e^{-\delta_{lj}A(f_a)} e^{-i2\pi\delta_{lj}[k(f_a)-f_a k'(f_a)]} S_j(a, b - \delta_{lj}k'(f_a)) \\ &= e^{-\delta_{lj}A(f_a)} e^{-i\delta_{lj}\phi_a} S_j(a, b - \delta_{lj}s_g(f_a)) \end{aligned} \quad (10)$$

where $\frac{\phi_a}{2\pi} \doteq k(f_a) - f_a k'(f_a) = f_a[s_\phi(f_a) - s_g(f_a)]$ appears as a phase factor multiplying the shifted CWT for sensor j.

Now note that from the above expression it follows that the phase factor is a function of both the group and the phase slowness and the modulus is related to the group slowness. This is intuitive as (a) the group slowness is related to the *energy* propagation, i.e. the velocity of propagation of the envelope and (b) the phase slowness is related to the velocity of propagation of the points of constant phase on the wavefront. Note that in the non-dispersive case the phase and the group slowness are the same. The relationships shown in equation (10) motivate the development of a modification of the Radon transform that is the basis of our method and which we describe in the next section.

IV. EXPONENTIALLY PROJECTED RADON TRANSFORM (EPRT)

To this end, let us fix a scale a and consider the array of CWT coefficients, $S_l(a,t)$ for each of the array waveforms at that scale where we now treat the shift as a time index t. The EPRT consists of two parts as applied to that array of CWT coefficients:

(a) Finding estimates $\hat{\phi}$ of the phase factor ϕ_a and $\hat{\alpha}$ of the attenuation $A(f_a)$ using the array of coefficients collected from a set of windows at a fixed *moveout* p.

(b) Using these estimates to apply a *modified* slant-stack (Radon transform) operation at moveout p on the collected array of CWT coefficients wherein we apply the projection operator $\mathbf{P}_u = \frac{1}{\sqrt{U^\dagger U}} U^\dagger$ onto the vector U given by

$$U = \begin{bmatrix} e^{-[\hat{\alpha}+i\hat{\phi}](z_1 - z_{l_0})} \\ \vdots \\ e^{-[\hat{\alpha}+i\hat{\phi}](z_L - z_{l_0})} \end{bmatrix}$$

instead of the simple sum operation in the regular slant-stack that corresponds to projecting on a vector of all 1's. l_0 is the reference receiver for stacking the waveforms. The result of this modified stacking operation is the output of the EPRT at scale p and window location t on the reference sensor.

We explain the above two steps further below.

IV-A. Estimation of phase and attenuation factors at a given moveout

Under the approximation in equation (10), we estimate the phase and the attenuation factors from the CWT coefficient array at a particular scale a and collected at a fixed moveout p as follows. Let us assume that we have the correct moveout $p = s_g$. Denoting $\delta_i = \delta_{il_0}$, we can write from equation (10)

$$\mathbf{Y}_a = \begin{pmatrix} S_1(a, t' + \delta_1 s_g) \\ \vdots \\ S_L(a, t' + \delta_L s_g) \end{pmatrix} = \begin{bmatrix} e^{-\delta_1(A(f_a)+i\phi_a)} \\ \vdots \\ e^{-\delta_L(A(f_a)+i\phi_a)} \end{bmatrix} S_{l_0}(a, t') + \mathbf{E}$$

where t' is a set of time indices in a window encompassing the mode of interest in the CWT domain at scale a and $\mathbf{E}$ is the error modeled as incoherent additive noise. In terms of notation $\mathbf{Y}_a$ is a $L \times |t'|$ matrix. To this end define

$$\begin{aligned} \mathbf{Y}_{a,1} &= [\mathbf{Y}_a(1)\ \mathbf{Y}_a(2)\ \cdots\ \mathbf{Y}_a(L-1)] \\ \mathbf{Y}_{a,2} &= [\mathbf{Y}_a(2)\ \mathbf{Y}_a(2)\ \cdots\ \mathbf{Y}_a(L)] \end{aligned}$$

where $\mathbf{Y}_a(i)$ is the i-th row of the matrix $\mathbf{Y}_a$. Now we compute the quantities,

$$R_{ij} = \mathbf{Y}_{a,j} \mathbf{Y}_{a,j}^\dagger \ i,j = 1,2$$

where $(\cdot)^\dagger$ denotes conjugate (Hermitian) transpose and we are therefore computing the inner product Note that $R_{ij} = R_{ji}^*$, so only one of them needs to be computed in practice. One can show that,

$$\begin{pmatrix} R_{11} & R_{12} \\ R_{21} & R_{22} \end{pmatrix} = \sigma_1 V^\dagger V + \sigma_2 I_{2\times 2}$$

where $I_{2\times 2}$ is the identity matrix of size 2 and σ_1 and σ_2 are positive constants. Now note that for a Uniform Linear Array (ULA) with inter-sensor spacing of δ, $V = [1\ e^{-\delta(\alpha+i\phi)}]$. We see that V is simply the right eigenvector corresponding to the dominant eigenvalue. Thus we have the estimates for ϕ and α as,

$$\hat{\alpha} = -\frac{1}{\delta} \log\left[\frac{\sqrt{(R_{11}-R_{22})^2 + 4||R_{12}||^2} - R_{11} + R_{22}}{2||R_{12}||}\right] \quad (11)$$

$$\hat{\phi} = -\frac{\angle(R_{12})}{\delta} \quad (12)$$

where $\angle(\cdot)$ is the angle (phase) of the complex argument.

For non-uniform arrays this process can be applied to the sensor array by selecting sensors that are at constant distance from each other or by simply applying this process to sensors in a pairwise fashion using the corresponding inter-sensor distance as δ for each pair and then taking the average.

IV-B. Exponentially projected slant-stack operation

Using the estimates of the attenuation and the phase factor as obtained in the previous step, we apply the projection operator $\mathbf{P}_U$ on the array data at scale a. For the sake of clarity of exposition, we will now assume a ULA. However the corresponding expressions can be developed for the general case as well and the method described here is not restricted by this assumption. The projection operator in the case of the ULA becomes,

$$\mathbf{P}_U = \left(\underbrace{e^{-\hat{\alpha}\delta(2l_0+1-L)} \frac{\sinh(\hat{\alpha}\delta)}{\sinh(L\hat{\alpha}\delta)}}_{=1/K}\right)^{1/2} U^*$$

Then the EPRT at scale a is the following transform,

$$\begin{aligned} &R_a(t, p; \hat{\alpha}, \hat{\phi}) \\ &= \frac{1}{K} \int_t^{t+T_w} \left| \sum_{l=1}^{L} e^{-(\hat{\alpha}-i\hat{\phi})\delta(l-l_0)} S_l(a, t + p(l-l_0)\delta) \right|^2 dt \end{aligned}$$

where we include the moveout, p, and window location, t, as primary arguments, and the estimated attenuation and phase as auxiliary arguments, and choose the window length, T_w, based on the scale being analyzed. The schematic of this operation is shown in figure 1. We can interpret this EPRT output as the normalized coherent energy (in the sense of conforming to the exponential propagation model) in the window given by the location and moveout across the array. Along the lines of [6] we can write a related quantity that we call the EPRT semblance as follows,

$$\begin{aligned} &\rho_a(t, p; \hat{\alpha}, \hat{\phi}) \\ &= \frac{1}{K} \frac{\int_t^{t+T_w} \left| \sum_{l=1}^{L} e^{-(\hat{\alpha}-i\hat{\phi})\delta(l-l_0)} S_l(a, t + p(l-l_0)\delta) \right|^2 dt}{\int_t^{t+T_w} \sum_{l=1}^{L} |S_l(a, t + p(l-l_0)\delta)|^2 dt} \end{aligned}$$

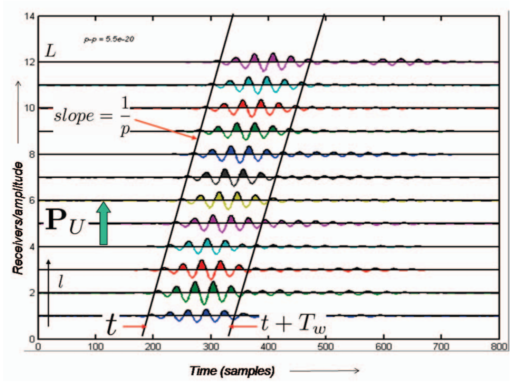

Fig. 1. Schematic representation of the EPRT with the reference receiver as the first receiver as applied to the CWT coefficients of the waveforms at scale a.

where we normalize the coherent energy described above by the total energy in the same window. This is therefore an indicator of fit to the exponential model with the best fit given by a value of 1.

IV-C. Overview of semblance analysis

Following the analysis in [6], assume that the time window length and location are chosen so as to enclose the coefficient waveform of interest completely. Then using Parseval's relation we can write,

$$\rho_a(p;\hat{\alpha},\hat{\phi}) = \frac{1}{K}\frac{\int\left|\sum_{l=1}^{L} S_l(a,f)e^{-(\hat{\alpha}-i(\hat{\phi}+2\pi pf))\delta(l-l_0)}\right|^2 df}{\int\sum_{l=1}^{L}|S_l(a,f)|^2 df}$$

where $S_l(a,f)$ is the Fourier transform of $S_l(a,t)$ and $\rho_a(p;\hat{\alpha},\hat{\phi})$ is the value of the semblance for a time window location chosen so as to encompass the signal appropriately. Then it follows from the linearity of the wavelet transform that,

$$S_l(a,f) = X(a,f)e^{-(A(f)+i2\pi k(f))\delta(l-l_0)}$$

where $X(a,f) = X(f)G^*(af)$. Plugging this expression into the expression for EPRT in the frequency domain we have,

$$\rho_a(p;\hat{\alpha},\hat{\phi}) = \tag{13}$$

$$\frac{\int\left|\sum_{l=1}^{L} X(a,f)e^{-(A(f)+i2\pi k(f))\delta(l-l_0)}e^{-(\hat{\alpha}-i(\hat{\phi}+2\pi pf))\delta(l-l_0)}\right|^2 df}{K\int|X(a,f)|^2\sum_{l=1}^{L}|e^{-A(f)\delta(l-l_0)}|^2 df}$$

We conduct our analysis by considering additional terms in the Taylor series expansions (8) and (9),

$$k(f) \approx s_\phi f_a + s_g(f-f_a) + \frac{s_g^{'}}{2}(f-f_a)^2$$
$$A(f) \approx A(f_a) + A'(f_a)(f-f_a)$$

For reasons of space, we show only the main result here, namely that the semblance of (13) is maximized by the following estimates

$$\hat{\alpha} = A(f_a) + A'(f_a)f_\delta \tag{14}$$

$$\hat{p} = s_g(f_a) + s_g^{'}\left(f_\delta + \frac{\Gamma_f^3}{2\Delta_f^2}\right) \tag{15}$$

$$\hat{\phi} = 2\pi\delta\left\{s_\phi(f_a)f_a - \hat{p}f_a + \frac{s_g^{'}}{2}\left(\Delta_f^2 - f_\delta^2 - \frac{\Gamma_f^3 f_\delta}{\Delta_f^2}\right)\right\} \tag{16}$$

which are given in terms of spectral moments defined by,

$$\Delta_f^2 = \frac{\int|\tilde{X}(a,f)|^2(\tilde{f}-f_\delta)^2 df}{\int|\tilde{X}(a,f)|^2 df};\Gamma_f^3 = \frac{\int|\tilde{X}(a,f)|^2(\tilde{f}-f_\delta)^3 df}{\int|\tilde{X}(a,f)|^2 df}$$

where

$$f_\delta = \frac{\int|\tilde{X}(a,f)|^2\tilde{f}df}{\int|\tilde{X}(a,f)|^2 df} \quad , \quad \tilde{f} = f - f_a \tag{17}$$

with $\tilde{X}(a,f) = \sqrt{\Pi(f)}X(a,f)$ where $\Pi(f) = \sum_{l=1}^{L}|e^{-A(f)\delta(l-l_0)}|^2$. The bias terms in equations (14-16) are small when the source spectrum does not exhibit steep dropoff over the spectral support of the wavelet at scale a.

Note that our method differs from the method in [4] in three major respects. First instead of searching over all the parameters we estimate the phase and attenuation and search only over group slowness. Second our method employs semblance as a criterion to estimate the parameters. In contrast to the energy based approach of [4], this makes it feasible to extract weak modes. Finally we explicitly deal with and estimate attenuation, which is an important parameter of interest in oilfield applications.

V. THE ALGORITHM

First we generate the CWT of the waveforms using a suitably chosen mother wavelet. We then select a reference sensor; this is usually taken to be the last one to maximize the temporal separation of interfering components. Then starting at the frequency (scale) that has the maximum energy the algorithm consists of the following steps for each frequency f_i (corresponding to scale a_i),

1. For each scale we use the time window length T_w based on the effective spread of the wavelet at that scale (dilation). This choice validates the analysis which assumes that the time window encompasses the signal at the scale a.
2. Pick a set of moveouts p corresponding to the expected range of group slowness.
3. For each of these moveouts shift and align the array of coefficient data corresponding to the moveout.
4. For these aligned arrays compute the estimates $\hat{\alpha}$ and $\hat{\phi}$ as described above.
5. Using these estimates construct a semblance map in the (t,p) domain. Locate the maximum on this map and declare the corresponding value of the moveout as the estimate $\hat{p}$.
6. Using continuity and smoothness of the dispersion curves, we speed up computation by limiting the search over the moveouts p at frequency f_i to be around a neighborhood of the moveout (slowness) value obtained at f_{i-1}.

The above process is repeated marching up in frequency, outputting the desired estimates at each step, thereby generating an estimate of the dispersion characteristic. The march up is terminated when the last frequency of interest is reached or when the maximized semblance falls below a threshold. The process is then repeated marching down from the starting frequency with a similar terminating condition.

The algorithm is depicted schematically in figure 2.

Multimode extraction: Note that if the modes are separated in time at scale a then the method and analysis easily extends to each of the modes with semblance peaks at different t in the $(t-p)$ plane.

V-A. Bias correction

When the source spectrum and the wavelet spectrum at a scale a are not aligned then there is a bias in the estimated dispersion parameters, given by equations (14-16). There are two ways to correct this bias:

1. **Frequency correction**: The bias in the estimation of both attenuation and slowness contains a linear term that is exactly the term in the first order Taylor series expansion evaluated at $f_a + f_\delta$. Assuming this dominates the other terms we can address the bias by declaring the estimates at f_a to be the estimates at $f_a + f_\delta$. This correction is readily obtained from the data and thus can be easily applied in one step.
2. **Slowness correction**: Alternatively we can explicitly estimate the bias terms that requires us to estimate the spectral moments from the data. However, the correction terms also involve estimation of the derivative of the group slowness. This requires a first pass

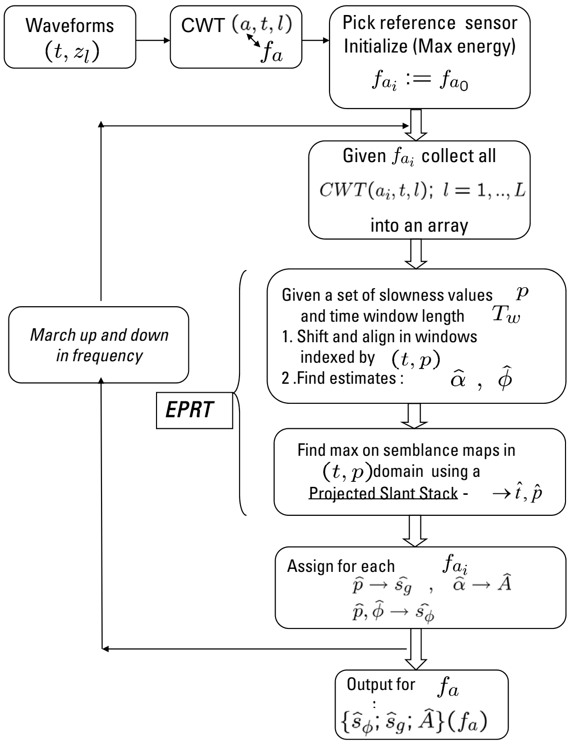

Fig. 2. The algorithm for dispersion extraction using EPRT.

to generate a (biased) group dispersion curve and then using a smoothing operator to estimate the desired derivative. The resulting correction is then applied to the estimated dispersion. This process can be iterated if necessary to refine the estimates.

VI. PERFORMANCE EVALUATION

For our experiments we choose the Morlet wavelet [5], because it is well matched with borehole acoustic data. We illustrate the performance of the proposed method for synthetic data in figure 3 and for real field data in figure 4. The former is generated using realistic model dispersion curves and include added noise. The model curves provide the ground truth which is matched very well after the bias correction. The real data example indicates the robustness and superiority of the new approach.

VII. CONCLUSIONS AND FUTURE WORK

In this paper we presented a wideband array processing method that works in the CWT domain for automatic dispersion extraction from a set of received waveforms. Experimental evaluation on both synthetic and real field data shows that the method is superior to existing methods and requires no post processing. Future work includes extending this to handle multiple modes, though for the non-overlapping case, one approach is briefly mentioned here.

VIII. REFERENCES

[1] J. Haldorsen, D. L. Johnson, T. Plona, B. Sinha, H. Valero, and K. Winkler, "Borehole acoustic waves," *Oilfield Review*, Spring 2006.

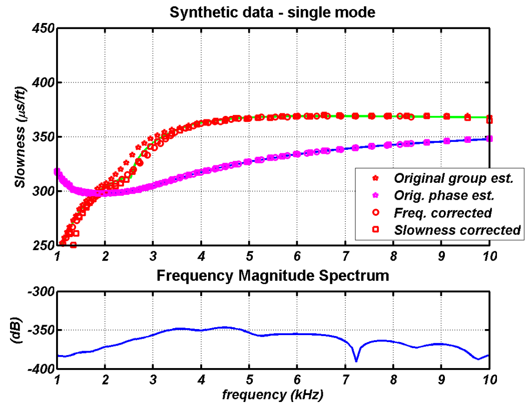

Fig. 3. Dispersion curve extracted using EPRT from synthetic data both with and without bias correction. The true model dispersion curves are also shown as solid lines and reveal the excellent match of the estimates to them.

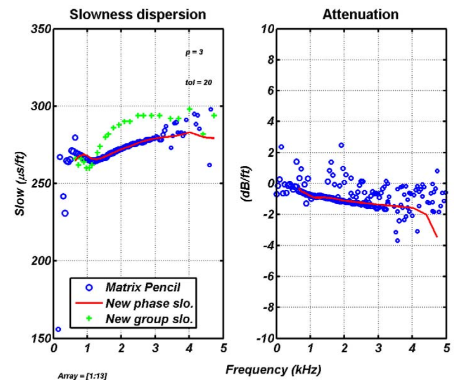

Fig. 4. An example of EPRT as applied to a frame of real field data acquired using a borehole sonic tool. Note the overall good match with existing matrix pencil algorithm for the phase slowness as well as the superior quality of the EPRT results as evidenced by smoother curves for both phase slowness and attenuation. The group slowness estimates are novel.

[2] S. Lang, A. Kurkjian, J. McClellan, C. Morris, and T. Parks, "Estimating slowness dispersion from arrays of sonic logging waveforms," *Geophysics*, vol. 52, no. 4, pp. 530–544, April 1987.

[3] M. P. Ekstrom, "Dispersion estimation from borehole acoustic arrays using a modified matrix pencil algorithm," ser. 29th Asilomar Conference on Signals, Systems and Computers, vol. 2, 1995, pp. 449–453.

[4] A. Roueff, J. I. Mars, J. Chanussot, and H. Pedersen, "Dispersion estimation from linear array data in the time-frequency plane," *IEEE Transactions on Signal Processing*, vol. 53, no. 10, pp. 3738–378, October 2005.

[5] A. Grossmann, R. Kornland-Martinet, and J. Morlet, *Wavelet, Time-frequency methods and phase space*, ser. Reading and understanding continuous wavelet transform, J. Combes, A. Grossmann, and P. Tchamitchian, Eds. Springer-Verlag, Berlin, 1989.

[6] C. Kimball and T. Marzetta, "Semblance processing of borehole acoustic array data," *Geophysics*, vol. 49, no. 3, pp. 264–281, March 1984.